Role of surface water molecules in stabilizing trapped hole centres in titanium dioxide (anatase) as monitored by electron paramagnetic resonance

Role of Surface Water Molecules in Stabilizing Trapped Hole Centres in Titanium Dioxide (Anatase) as Monitored by Electron Paramagnetic Resonance

Enzo Gabriele Panarelli[a], Stefano Livraghi[b]*, Sara Maurelli[b], Valeria Polliotto[b], Mario Chiesa[b] and Elio Giamello[b].

a Huygens-Kamerlingh Onnes Laboratory, Department of Physics, Leiden University, P.O. Box 9504, 2300 RA Leiden, The Netherlands

b Dipartimento di Chimica, Università di Torino and NIS centre, Nanostructured Interfaces and Surfaces, Via P. Giuria 7, 10125 Torino, Italy

Stefano Livraghi: stefano.livraghi@unito.it

Key words: EPR, ENDOR, TiO_2, trapped holes, water.

Abstract.

A key factor affecting the photo-efficiency of TiO_2 is strictly related to the fate of charge carriers, electrons (e^-) and holes (h^+), generated upon band gap excitation. In the present paper we point our attention to the nature of the hole trapping sites in the anatase polymorph monitored coupling the conventional continuous wave EPR (CW-EPR) technique with pulse electron nuclear double resonance (ENDOR) experiments. the attention is focused on the role of surface adsorbed water (both in molecular and in dissociated form) in the stabilization of photogenerated hole centres.
CW-EPR results indicates that two distinct $O^{\bullet-}$ hole centres can be identified in Anatase ($O^{\bullet-}_{surf.}$ and $O^{\bullet-}_{subsurf.}$) and that the quantitative ratio (measured in terms of spectral intensity) of these two species is markedly conditioned by the presence of surface physisorbed water. For the first time a h^+-proton distance, evaluated via ENDOR measurement, is reported.

1. Introduction

Titanium dioxide (TiO_2) is by far one of the most widespread photocatalysts, of importance in several technological fields.[1] A key factor affecting the photo-efficiency of TiO_2 is strictly related to the fate of charge carriers, electrons (e^-) and holes (h^+), generated upon band gap excitation. While a large portion of the photogenerated charge pairs instantly recombine, a fraction

can diffuse towards the surface. Surface trapped electrons and holes can then recombine or act as initiators for subsequent processes occurring at the surface.[2] In the absence of reactive molecules at the interface (i.e. for a system kept under vacuum) the charge carriers are stabilized respectively as Ti^{3+} ($Ti^{4+} + e^- \rightarrow Ti^{3+}$) and $O^{\bullet-}$ ($O^{2-} + h^+ \rightarrow O^{\bullet-}$) that are two paramagnetic species and have been observed by Electron Paramagnetic Resonance spectroscopy (EPR). A key aspect for the photoactivity of titanium dioxide is the role of water adsorbed at the surface. Water adsorbed on TiO_2 can play a dual role, acting as promoter or as inhibitor of the photocatalytic process, depending on the experimental conditions.[3,4] The inhibition aspect is strictly related to the role of water as a site blocker,[5,6] while the promoting effect is related to its role as a source of $OH^{\bullet}$ species.[7] The photo oxidation processes on TiO_2 in fact can occur as a consequence of direct hole (h^+) transfer or through $OH^{\bullet}$ radical species.[8] However, there is no general consensus on the mechanism leading to this last species. The $OH^{\bullet}$ in fact can be generated either via direct hole trapping by surface OH^- groups ($h^+ + Ti(O\text{-}H)^- \rightarrow Ti(O\text{-}H)^{\bullet}$) or via hole transfer to water ($H_2O + h^+ \rightarrow OH^{\bullet} + H^+$). Alternatively it can be formed as a result of electron scavenging by dissolved oxygen with formation of hydrogen peroxide as intermediate ($O_2 + 2H^+ + 2e^- \rightarrow H_2O_2 + h\nu \rightarrow 2OH^{\bullet}$).[9,10] The capability to monitor the charge carrier localization within the oxide, and the role of adsorbed water on the carriers' fate, represents a key step to understand and selectively control the properties of titanium dioxide, with the final aim of reducing the undesired charge recombination in photocatalytic phenomena.

As far as the positive carriers are concerned, many experimental and computational studies, have been performed to determine the nature and the localization of photogenerated trapped holes in titanium dioxide. Experimental evidence shows that oxidation sites are preferentially located at the (001) crystallographic face of anatase (the preferential face for rutile is the (111)) .[11,12,13] It is also generally accepted that holes can be trapped to form $O^{\bullet-}$ centres, but there is no general consensus about the nature and location of the trapping site. Surface oxygen radical centres or alternatively sub-surface ones located in proximity of surface hydroxyl groups have been reported.[2,7,14] In the case of the rutile polymorph the stabilization of holes in sub-surface positions has been also recently suggested by theoretical studies.[15,16]

Since charge carriers bear one unpaired electron, EPR spectroscopy represents a powerful technique to get information about the nature and localization within the solid of such species. In the literature a large bulk of EPR data related to trapped electrons (usually associated with Ti^{3+} ions) is available, while a relatively lower number of papers is devoted to the characterization of trapped hole centres.[17,18,19,20,21,22,23,24,25,26,27]

EPR spectroscopy allowed identifying two distinct signals ascribable to trapped hole centres.[14] In 1987 R. Howe and M. Grätzel[18] reported EPR evidence of trapped holes in TiO_2 generated upon irradiation of a hydrated anatase. Since the observed EPR signal of the hole centre (characterized by g_1=2.016, g_2=2.012 and g_3=2.002) was not affected by the presence of O_2, it was assigned to a sub-surface $O^{\bullet-}$ centre and the following notation $Ti^{4+}O^{\bullet-}Ti^{4+}OH^-$ was proposed.[17] In 1993 Micic *et al*. observed a hole centre with principal *g* values g_1=2.027, g_2=2.018 and g_3=2.003. The corresponding paramagnetic centre was described as a surface trapped hole formed by the following mechanism: $h^+ + Ti^{4+}O^{2-}Ti^{4+}OH^- \rightarrow Ti^{4+}O^{2-}Ti^{4+}O^{\bullet-} + H^+$.[18]

Later in 1997, Y. Nakaoka and Y. Nosaka studied the dependence of the EPR features of trapped holes in TiO_2 samples calcined in air at different temperatures. In this case the authors were able to identify two distinct types of hole centres. The former (g_1=2.018, g_2=2.014 g_3=2.004) is similar to that reported by R. Howe[18](see before), while the second one (g_1=2.030, g_2=2.018 and g_3=2.004) is close to those reported by Micic *et al*.[18] and ascribed by the authors to a surface hole centre.[19] Quite similar results were also reported by H-H. Lo *et al*.[20] and by N.M. Dimitrijevic *et al.* who studied the dependence of the EPR signals of trapped charge carriers on the shape and size of the anatase crystals.[21] By combining pulse EPR measurements with the classic continuous wave EPR experiments (CW-EPR), the authors concluded that the **g** tensor of oxygen-centred radicals (g_1=2.024, g_2=2.014, g_3=2.007) was independent from the size and shape of the TiO_2 microcrystals, while the transverse relaxation time (T_2) of surface-trapped holes ($O^{\bullet-}_{surf.}$) was affected by the presence of surrounding protons.[21]

The picture emerging from the above mentioned EPR results, in spite of some non-negligible contradiction, points to the existence of two families of trapped hole centres in anatase. These two families differ essentially in the value of the higher g component (classically indicated as g_x at low magnetic field) which, as it will be shown later, is the most sensitive to the surrounding crystal field. The g_x of the first family lies in the range 2.016-2.018, while the g_x of the second family lies at higher values, in the range 2.024-2.030. However, a general consensus on the location and on the structural features of these two kinds of centres is still missing.

Recently we have published a series of papers devoted to the rationalization of the EPR signals of trapped electrons (Ti^{3+}) in all the main polymorphs of TiO_2.[28,29,30,31] In the present paper we turn our attention to the nature of the hole-trapping sites in anatase, coupling the conventional continuous wave (CW) EPR technique with pulse electron nuclear double resonance (ENDOR) experiments focusing, in particular, on the role of surface-adsorbed water (both in molecular and in dissociated form) in stabilizing the hole centre.

2. Materials and Methods

2.1 Sample preparation

TiO_2 anatase was obtained via sol-gel synthesis, as described in a previous work.[32] Briefly, a titanium(IV) isopropoxide ($Ti(OC_3H_7)_4$) solution in 2-propanol (molar ratio 1:4) was reacted with water (molar ratio between alcohol and water 1:10) under constant stirring at room temperature. The obtained gel was aged overnight at room temperature (RT) to ensure the completion of the hydrolysis and was subsequently dried at 343 K. The dried material was eventually calcined at 773 K in air (heating rate 10 K/min) for 2 h. Basic structural, morphological and optical characterization of the as prepared material are reported as Supporting Information.

Two main types of TiO_2 specimens were employed in the spectroscopic investigation: an activated sample (ac-TiO_2) and an as-prepared one (ap-TiO_2). In the first case the sample was outgassed under high vacuum (residual pressure $< 10^{-4}$ mbar) at 773 K for 0.5 hours in order to remove adsorbed water, surface hydroxyl groups, and other surface impurities. Then oxidation with 20 mbar of O_2 was performed at the same temperature for 1 h to obtain a fully oxidized, stoichiometric oxide. The samples were then cooled to room temperature under O_2 atmosphere, and the gas phase was eventually removed at this temperature down to a residual pressure of 10^{-4} mbar. Samples prepared via this standard procedure will be indicated in the text as "activated" or ac-TiO_2.

The two kinds of TiO_2 systems considered in this work (activated and as-prepared TiO_2, respectively) differ in terms of the state of the surface. Previous careful studies on the hydration-dehydration of the anatase surface have clarified that the surface of the activated material, due to the high outgassing temperature, is free from both adsorbed water and hydroxyl groups. In contrast, the as-prepared material is partially hydroxylated (in particular the (100) surface) and also contains some adsorbed molecular water not eliminated by room temperature outgassing [33]

Samples prepared by simply outgassing the calcined material at RT will be referred to in the following as "as prepared" (ap-TiO_2).

2.2 EPR characterization

For the spectroscopic characterization of all the samples a quartz tubular cell allowing *in situ* EPR measurements was employed. Trapped holes were generated upon *in situ* irradiation of the samples for 5 seconds at T = 77K into the EPR cavity using a 1600W Xe Lamp (New Port Instruments) equipped with a IR water filter. Such irradiation time was chosen because it represents the optimal condition for monitoring the trapped holes. In fact, although at 77K the EPR signals of

the trapped holes, in both activated and as-prepared TiO_2 are stable for several hours, longer irradiation time causes a decrease of the EPR intensity likely due to the electron-hole recombination (see S.I.) X-band CW-EPR spectra were detected at 77 K on a Bruker EMX spectrometer (microwave frequency 9.46 GHz) equipped with a cylindrical cavity. A microwave power of 1 mW, a modulation amplitude of 0.2 mT and a modulation frequency of 100 KHz were used. Pulse EPR experiments at X-band (9.76 GHz) were performed on an ELEXYS 580 FT-EPR Bruker spectrometer equipped with a liquid-helium cryostat from Oxford Inc. The magnetic field was measured by means of a Bruker ER035 M NMR gauss meter.

X-band Electron-Spin-Echo- (ESE) detected EPR experiments were carried out with the pulse sequence: $\pi/2–\tau–\pi–\tau–echo$. Microwave pulse lengths $t_{\pi/2}$ = 16 ns and t_{π} = 32 ns and a τ value of 200 ns were used. A 1 kHz repetition rate was used.

Mims ENDOR spectra were measured with the mw pulse sequence $\pi/2–\tau–\pi/2–T–\pi/2–\tau–echo$ with $t_{\pi/2}$ = 16 ns. The time τ was 250 ns. During the time T a radio frequency pulse was applied, the length of which has been optimized for ^1H by a nutation experiment. Optimal length was found to be 12 μs. The temperature adopted for the ENDOR experiments was 15 K. A shot repetition rate of 1 kHz was used. In order to increase the signal-to-noise ratio, 50 scans were run and the spectra added together.

EPR signal intensity was obtained via double integrations of the spectra using Win-EPR software. EPR spectra were simulated using the EasySpin program.[34]

3. Results and Discussion.

CW-EPR spectra of the two types of anatase TiO_2 samples recorded after UV irradiation under vacuum are reported in Figure 1. The as-prepared material (ap-TiO_2, containing surface adsorbed water) shows a complex EPR pattern centered at g values typical of trapped hole centers, $O^{\bullet-}$, in TiO_2 (Figure 1a). Computer simulation of the experimental spectra allowed to identify two distinct signals contributing to the spectrum, indicated as species A and species B respectively which contribute to the overall intensity of the spectrum for about 35% and 65% respectively (stick-diagrams in Figure 1a). Beside the spectrum of trapped holes, a broad signal at higher field is also observed, which is due to trapped electrons (not shown in fig. 1).

Both signals of trapped holes (A and B) are characterized by a rhombic **g** tensor with a different degree of anisotropy, that is more pronounced in the case of signal B (Table 1). The irradiation experiment has then been performed on the same ap-TiO_2 sample kept under oxygen at 77K and thus covered by a physisorbed layer of O_2 atmosphere. In this case the EPR spectrum is drastically simplified showing the signal of species A only (Fig. 1b). This indicates a different

response of the two paramagnetic species (A and B) to the presence of physisorbed oxygen. The effect of surface adsorbed oxygen on paramagnetic centers is well known. Since O_2 is a paramagnetic molecule (S=1) a dipolar interaction occur between the molecules in the ad-layer and the paramagnetic centers underneath causing a strong broadening of the EPR signal which actually vanishes. The same result reported in Fig. 1b is obtained by contacting the surface of ap-TiO_2 sample with pure O_2 at 77 K after the trapped holes have been generated (Fig. 2). In fact, upon contacting the photogenerated trapped holes with oxygen at low temperature in dark condition, the spectrum of species B is not detectable anymore, thus disclosing the features of species A.

Irradiation of the activated, fully dehydrated ac-TiO_2 sample (Fig. 1c) produces the same result observed in the previous case (hydrated sample under oxygen, Fig. 1b), consisting of the presence of the signal of species A only. Actually, in the case of Fig. 1c, species A is the only one formed, whereas in the previous case (Fig. 1b) species A and B are both generated and the second one is canceled by the interaction with oxygen. The signal of species A in Fig. 1c (not affected by O_2) has a lower intensity (about one third) of that observed for the as-prepared sample reported in Figure 1b. The g values of the two species derived from computer simulations are listed in Table 1.

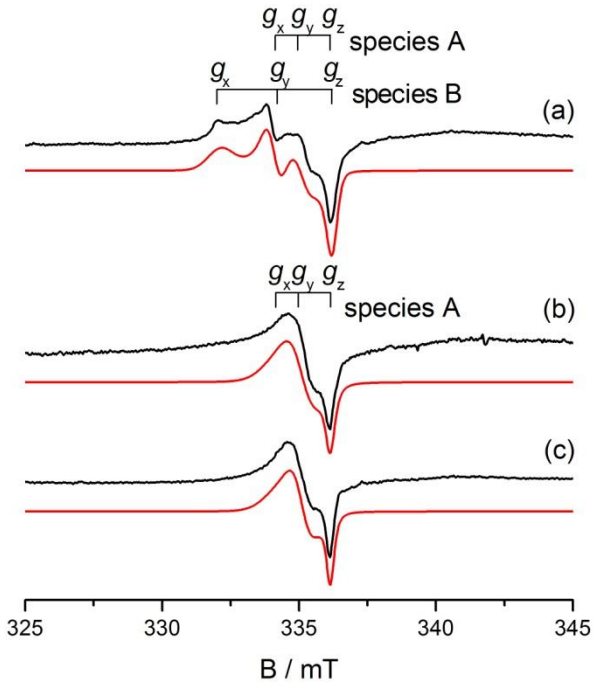

Figure 1. Normalized CW-EPR spectra (black lines) of hole centers in UV-irradiated anatase at 77 K, and corresponding computer simulations (red lines): (a) as-prepared sample (ap-TiO_2) irradiated under vacuum; (b) the same sample irradiated under O_2 atmosphere; (c) activated sample (ac-TiO_2) irradiated under vacuum. The spectra are recorded at T = 77 K after irradiation for 5 seconds at the same temperature. Each experimental spectrum is the result of three scans.

In synthesis, two distinct types of trapped hole $O^{\bullet-}$ centers (A and B) have been observed upon irradiating anatase under vacuum. The former is present on both hydrated and dehydrated surfaces

and is O_2-insensitive, whereas the other type (species B) is observed on hydrated surfaces only and its EPR signal reversibly vanishes upon O_2 physisorption. This indicates that species B is more exposed at the surface than species A.

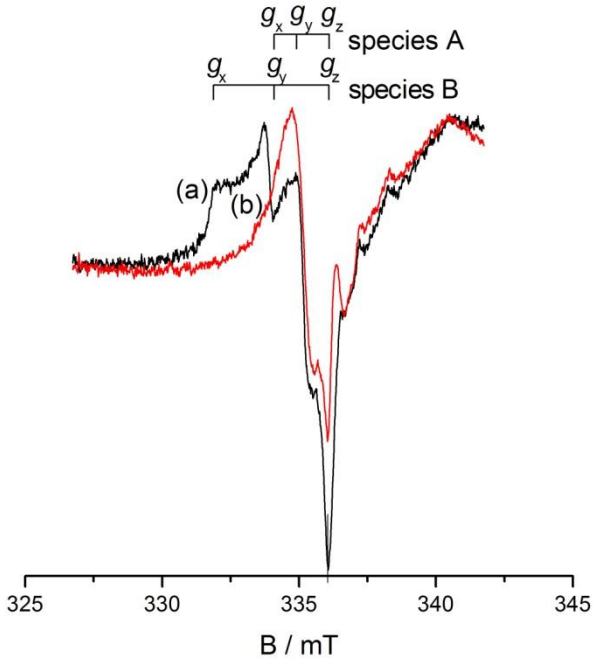

Figure 2. CW-EPR spectra of ap-TiO_2 after UV irradiation at 77K (a) and after contact with O_2 at 77 K(b).

	g_x	g_y	g_z
Species A	2.016 ± 0.005	2.011 ± 0.005	2.005 ± 0.002
Species B	2.029 ± 0.002	2.017 ± 0.002	2.004 ± 0.002

Table 1. Spin-Hamiltonian parameters extracted from the computer simulations of the CW EPR spectra of Figure 1.

In order to test the reactivity of the photogenerated hole centres, the solid has been contacted with molecular H_2 (Fig. 3).[35] Hydrogen is known to be a hole scavenger that reacts with an $O^{\bullet-}$ ion accessible from the surface generating an H atom:

(1) $O^{\bullet-}_{surf.} + H_2 \rightarrow OH^-_{surf} + H^\bullet$

The H atom immediately ionizes, injecting an electron into the solid:

(2) $H^\bullet + O^{2-}_{surf} \rightarrow OH^-_{surf} + e^-$.

The electron is then trapped by the cationic sites, forming a Ti^{3+} centre easily observed by EPR.

(3) $Ti^{4+} + e^- \rightarrow Ti^{3+}$

We show in Figure 3 the EPR spectra of the photo-irradiated TiO_2 samples before and after reaction with 10 mbar of H_2 (ac-TiO_2 sample in panel A and ap-TiO_2 in panel B). Inspection of the

figure shows that upon reaction with H_2 the EPR signal of the hole centres is partially depleted, while the signal due to Ti^{3+} centres increases in agreement with equations 1 – 3. In the experimental conditions adopted, however, the holes are not completely consumed by gaseous hydrogen. Fig. 3 also shows that both A-type and B-type hole centres react with H_2. In both cases, before and after H_2 contact, the overall EPR intensity is almost equal, indicating that the consumed hole centers roughly correspond to the growth of the Ti^{3+} centers. The experiment described in Fig. 3 thus suggests that both types of hole centres are at the surface or sufficiently close to it to react with hydrogen in the gas phase.

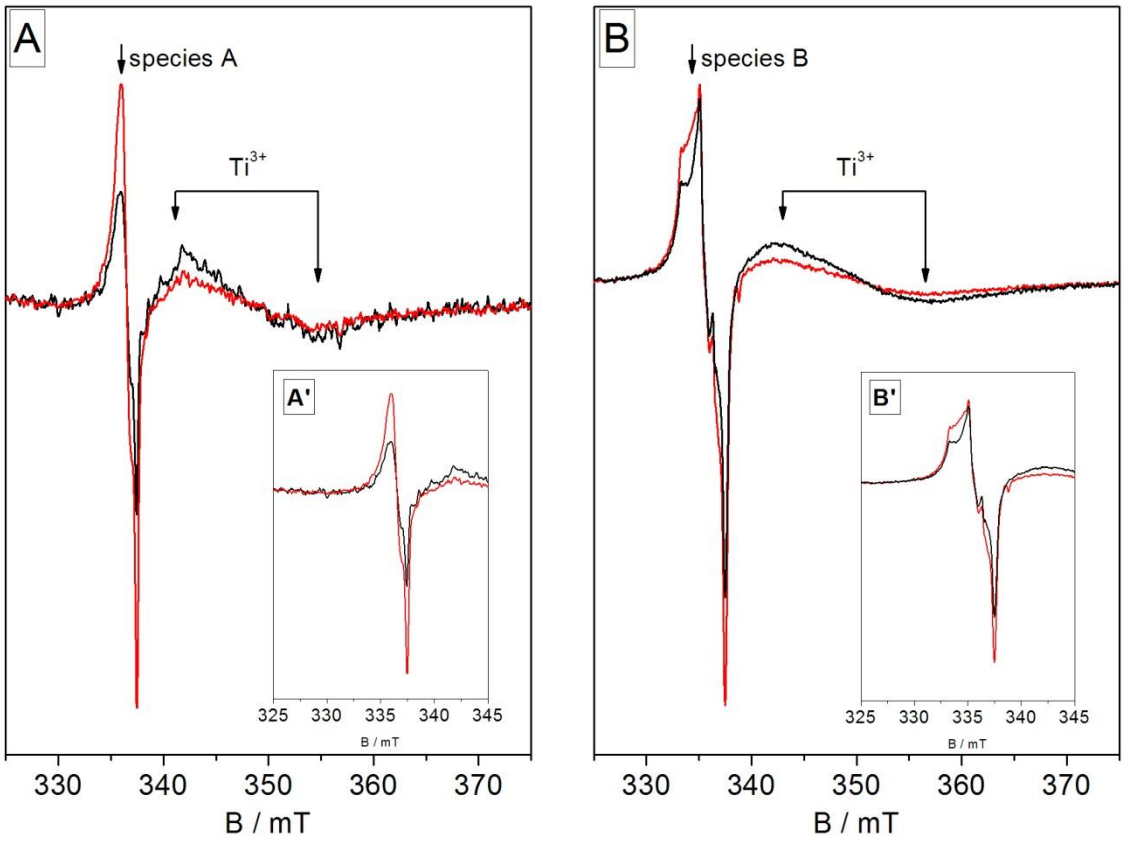

Figure 3. CW EPR spectra of activated (panel A) and as-prepared TiO_2 (panel B). The spectra are recorded at T = 77 K after UV irradiation for 5 seconds (red line) and subsequent contact with 10 mbar H_2 at the same temperature (black line). The corresponding insets A' and B' show a magnification of the hole signals.

3.1 Role of adsorbed water on hole-trapping centres.

In order to further clarify the nature of the two hole species identified in the EPR spectra of Figure 1, we performed specific experiments that monitor the effect of irradiation on samples outgassed *in vacuo* at increasing temperatures. The adopted annealing temperatures have been selected on the basis of literature results.[33] The EPR spectra of irradiated TiO_2 samples previously outgassed at increasing temperature (353 K and 423 K) are shown in Figure 4. In Figure

4(a) the spectrum of the irradiated as-prepared sample (previously outgassed at RT) is reported for sake of comparison. The EPR spectrum of the sample evacuated at T = 353 K for 30 minutes (Fig. 4b)remains qualitatively unaltered, even if the overall spectral intensity drops to about one third of the initial one (inset of Fig. 4). On the contrary, when the sample is outgassed at 423 K, the irradiation produces the sole species A and the whole intensity further drops to one tenth of the initial one (Figure 4c).

Based on the FTIR experiments reported in ref. 33, by outgassing at T = 353 K only a fraction of the adsorbed water is removed, while at 423 K only few hydroxyl (–OH) groups are left on the surface. The progressive decrease of the spectral intensity with increasing the evacuation temperature (inset of Figure 4) indicates that the presence of molecular water favours the stabilization of trapped holes on the anatase surface. It is worth noting that the initial signal corresponding to the two species A and B (Fig. 4a) can be restored if the material, outgassed at 423 K, is re-irradiated after a simple contact with water vapor pressure (see S.I.).

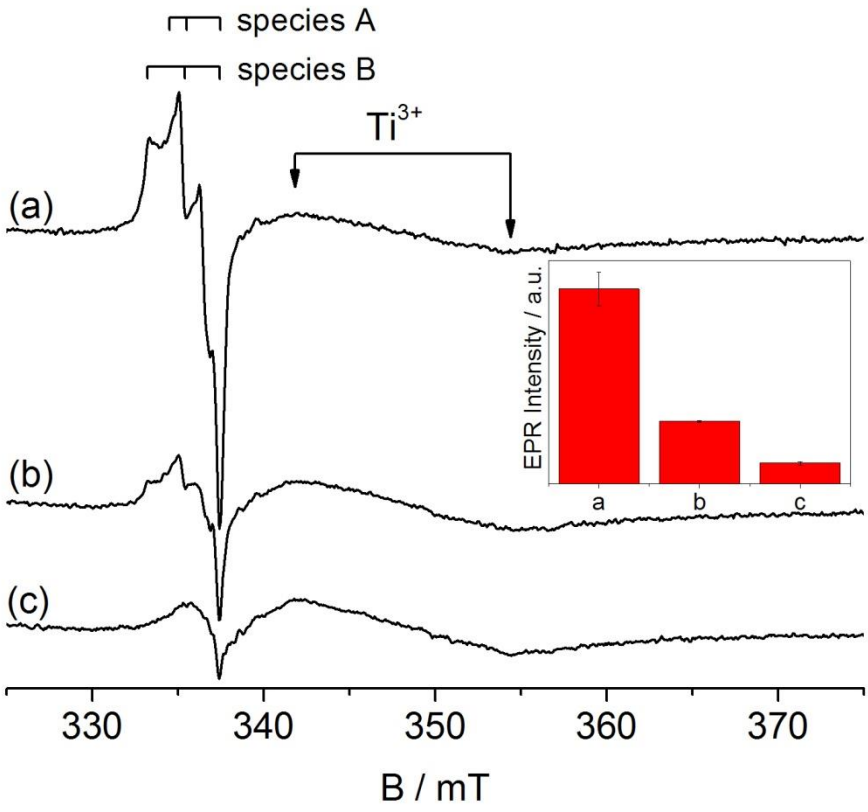

Figure 4. CW-EPR spectra of TiO_2 samples irradiated with UV after outgassing at different temperatures: (a) short evacuation at room temperature (as-prepared); (b) 30 minutes evacuation at 353 K; (c) 30 minutes evacuation at 423 K. The EPR spectra are recorded at T = 77 K upon 5 seconds of UV irradiation at the same temperature. The inset reports the EPR intensity obtained via double integration of the hole signal.

Advanced EPR methods, in particular the so-called hyperfine techniques (HYSCORE and pulse ENDOR), can provide invaluable information about the localization and the chemical

environment of paramagnetic species of importance in catalytic reactions.[29,36] In order to ascertain the local environment of species B, ENDOR experiments were performed. ENDOR is a powerful technique to detect the hyperfine interactions of unpaired electrons with magnetically active nuclei, with MHz resolution. Figure 5 shows pulse ENDOR spectra recorded with the Mims sequence at magnetic field settings corresponding to the principal **g** tensor values of the EPR spectrum of the hole centre.

The experiments were performed in order to detect the hyperfine interaction (if any) with the protons (I=1/2) present on the TiO_2 hydroxylated surface. The spectra are dominated by a weak signal centered at the proton Larmor frequency (~14.9 MHz) characterized by a maximum spectral extension of about 2.5 MHz. The ENDOR spectra recorded at different field positions of the EPR spectrum (Figure 5 (a)-(d)) do not show a marked dependence of the proton coupling tensor on the external magnetic field.

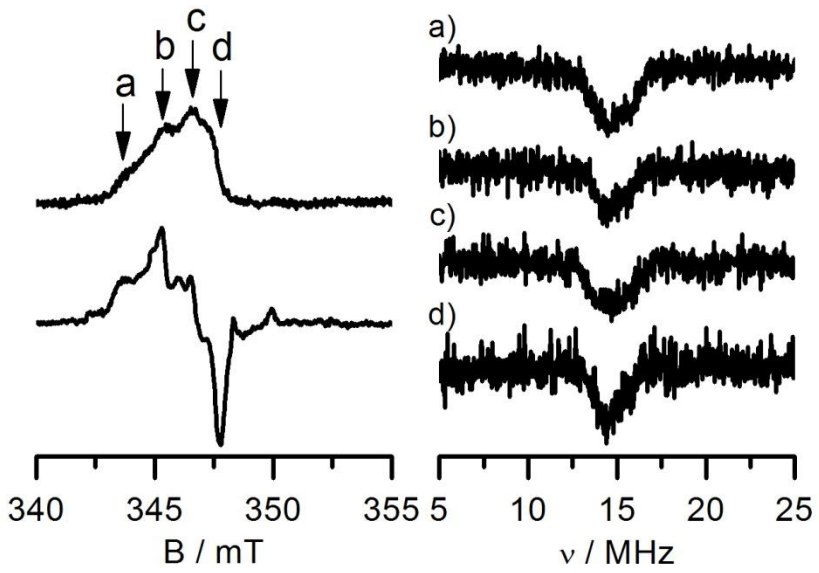

Figure 5. Left-hand side: ESE detected EPR spectrum of trapped hole in anatase sample outgassed at RT (upper spectrum) and corresponding first derivative (lower spectrum). The arrows indicate the magnetic field positions at which the ENDOR spectra were recorded. Right-hand side: ^{1}H Mims ENDOR spectra recorded for the as-prepared TiO_2 sample kept under vacuum recorded upon 5 seconds of UV irradiation. The spectra were recorded at T = 15 K and field positions indicated by the arrows: (a) 344.6 mT, (b) 345.7 mT, (c) 346.7 mT, (d) 347.8 mT.

The reason of this fact can be attributed to the small **g** anisotropy of the EPR spectrum that, together with the broad line-width due to the typical heterogeneity of a polycrystalline material , affects the spectral resolution. Assuming that the hyperfine interaction is dominated by the anisotropic term *T* and adopting a purely point–dipolar approximation , the distance *r* between the proton and the $O^{\bullet -}$ radical can be estimated from equation (4):

$$T = \frac{\mu_0}{4\pi} g_e g_n \beta_e \beta_n \frac{1}{r^3} \qquad (4)$$

Where μ_0 is the magnetic susceptibility, g_e and g_n the electron and nuclear g factors, respectively, β_e the Bohr magneton and β_n the nuclear magneton. The distance r, calculated in this way, is found to be of the order of 0.32 nm.

3.2 Nature of hole trapping centres.

The expected structure of the **g** tensor for the $O^{\bullet-}$ radical ion (electron configuration $2p_x^2$, $2p_y^2$, $2p_z^1$) has been discussed years ago by Brailsford *et al*.[37] In the most general case of rhombic symmetry and neglecting second order terms, the **g** tensor can be described by the formulas reported in Scheme 1, in which the parameters are the spin orbit coupling constant (λ), that for atomic oxygen amounts to 135 cm^{-1}, and the energy differences ΔE_1 and ΔE_2 corresponding to the separation between the $2p_z$ and the other two p orbitals induced by crystal field effects.

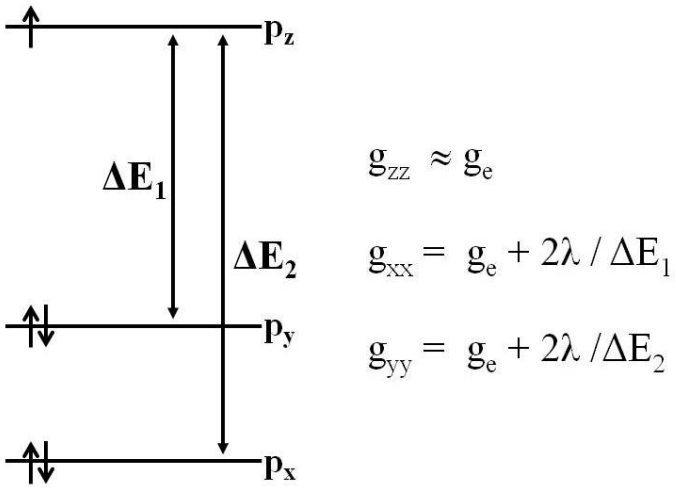

Scheme 1. Crystal field effects on a O^- radical ion. Adapted from Ref. 37.

On the basis of the experimental results reported in this work the following considerations can be drawn. In TiO_2 anatase irradiated under vacuum, two different EPR signals originating from trapped holes ($O^{\bullet-}_{surf.}$) are identified, both characterized by a rhombic **g** tensor. However, the degree of rhombicity is different in the two species, and is more pronounced in the case of species B ($O^{\bullet-}_B$) whose g_{xx} and g_{yy} values (the two crystal-field-sensitive components) are larger than those of species A ($O^{\bullet-}_A$, Table 1). This means that the energy splitting terms (ΔE_1 and ΔE_2) are smaller in the case of $O^{\bullet-}_B$. Since the crystal field acting on a surface species is weaker than the one felt by a bulk species, the **g** tensor observed for $O^{\bullet-}_B$ is consistent with the description of this species in terms of a surface hole center ($O^{\bullet-}_{surf.}$), based on the observed dipolar broadening of the signal under adsorbed oxygen (Fig.s 1b and 2). Taking into account that the photogenerated holes in

anatase are thought to be preferentially trapped at the (001)-surface[12,13], we consider the structure of this very surface for the assignment of the observed species. The (001) face of anatase has been investigated by experimental and computational tools.[38-,39,40] The termination of such a surface consists of protruding oxygen ions which are two-coordinated because they bridge two Ti^{4+} ions. Recalling that the oxygen ions in the bulk of anatase are only three-coordinated, and since a single coordination of an O^{2-} ion at the surface appears quite implausible, we can tentatively assign the EPR signal of the $O^{\bullet-}_B$ hole centre to a two-coordinated oxygen most probably located at the (001) face.

The second species ($O^{\bullet-}_A$) is located under the surface. The signal of this species is consistently less anisotropic than that of $O^{\bullet-}_B$ (higher crystal field around the centre) and is not affected by physisorbed oxygen (Fig. 2b). However, at least a fraction of the $O^{\bullet-}_A$ species must be located not very far away from the surface, as indicated by the fact that it appears accessible to hydrogen molecules. Since we have shown that $O^{\bullet-}_B$ is very likely two-coordinated, it is more than reasonable to describe $O^{\bullet-}_A$ as a three-coordinated (bulk) centre. A fraction of these centres is located in the immediate surroundings of the surface ($O^{\bullet-}_{subsurf.}$) and is accessible to H_2. (Fig. 3). A second important information derived from the present work concerns the role played by surface water in the stabilisation of the photogenerated holes. The most abundant production of stable hole centres is in fact observed when both surface hydroxyl groups and physisorbed water are present on the anatase surface (Fig. 4). The intensity of the hole spectra in fact decreases moving to a simply hydroxylated surface (Fig. 4) and decrease further in case of a fully dehydrated material (Fig. 4). The $O^{\bullet-}_{surf.}$ species, in particular, is not observed in the absence of physisorbed water.

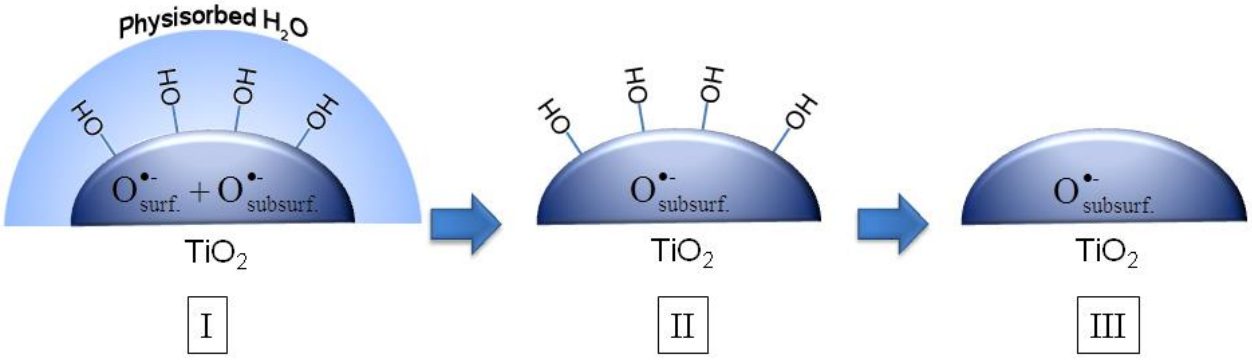

Figure 6. Sketch representing the effect of physisorbed water and surface OH groups on the EPR signal of trapped holes in TiO_2 anatase. I) hydroxylated material in the presence on physisorbed water (as-prepared sample). II) hydroxylated sample (as-prepared sample outgassed at 423 K). III) fully dehydroxylated sample (activated sample).

Anyway, the role of water (both in the molecular and in the dissociated state) in the stabilisation of the hole centres does not, however, involve the close contact with the paramagnetic centres. The ENDOR experiments here reported, in fact, have allowed the evaluation of the typical

$O^{\bullet-}_{surf.}$--H distance which amounts to 0.32 nm. This distance is compatible, considering the case of chemisorbed water, with the separation occurring between the oxygen hosting the hole and a proton is relatively large and such distance roughly corresponds, considering the fully stoichiometric (001) face, to the second coordination shell. (sphere evidenced in Fig. 7). Also in the case of protons belonging to physisorbed water molecules, however, they actually are relatively far away.

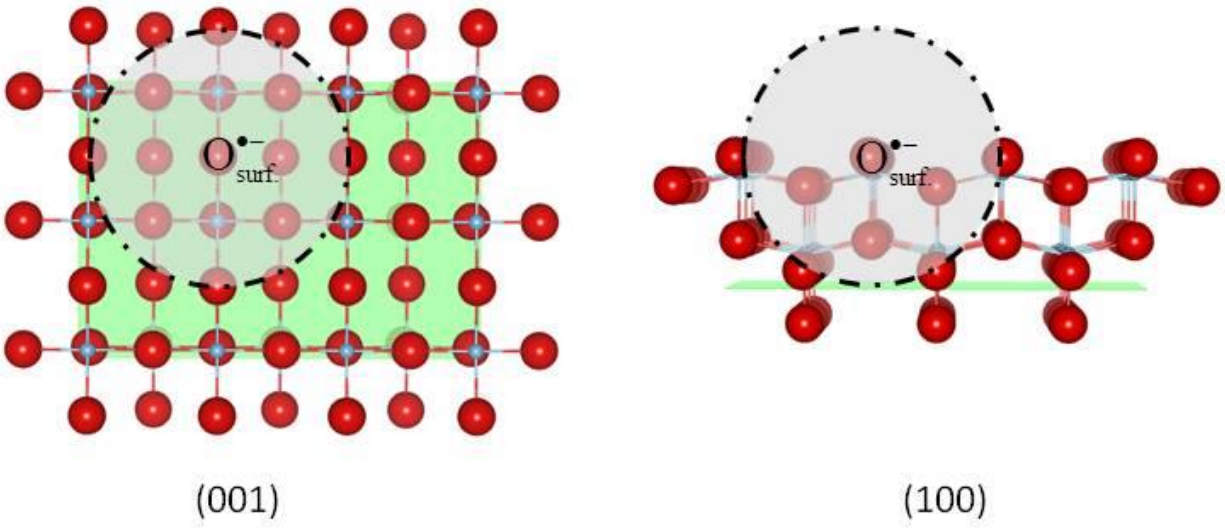

Figure 7. Graphical representation of the TiO_2 (001) and TiO_2 (100) faces for the anatase polymorph and the trapped hole – proton interaction radii (gray spheres, r = 0.32 nm), estimated via ENDOR measurements for surface oxygen. The green plane represents the orientation of the (001) face in the two structures. The structures are rearranged from Ref.[41]

The model arising from the data here discussed is thus that of a relatively abundant stabilisation of surface hole centres occurring in the case of the presence of a sort of nest composed by hydroxyl groups and water molecules (see Fig 6-I) which surround the hole centre itself. At the present stage of this work, is not possible to more accurately describe site corresponding to species B. The observed distance (0.32nm) [42,43] however seems to exclude a site consisting in a trapped hole at a flat surface with physisorbed water molecules. In this case, in fact, computer modelling available in the literature predicts distances between H and surface oxygen (hydrogen bonding) lower than 0.3 nm.[41,42]. The real (polycrystalline) sample used in the present work show a complex morphology (see TEM image in the S.I.) that cause these materials to markedly differ from the flat-free ideal surface. A computational approach to the present results needs the use of a more complex models of the surface (steps, hydroxyl groups, etc.)

4. Conclusion.

The formation of trapped hole centres ($O^{\bullet-}$) photogenerated by UV irradiation of polycrystalline anatase at low temperature has been monitored by EPR techniques (CW-EPR and Pulsed-ENDOR).

Two families of $O^{\bullet-}$ species (surface and sub-surface ones having different coordinative environment) have been put into evidence on the basis of their spectral features and of their behaviour upon contact with various adsorbates. We have also put into evidence the role of water in stabilizing the surface hole centers which need the presence of a complex environment composed by both surface hydroxyl groups and less close physisorbed water molecules. This observation is relevant for the comparison of the mechanisms of photocatalytic reactions performed in water suspensions (the large majority) and those performed under a gas phase.

Acknowledgements.

This work has been supported by the CARIPLO Fondation through the grant n° 2013-0615 "Novel heterojunction based photocatalytic materials for solar energy conversion" The support of the COST Action CM1104 “Reducible oxide chemistry, structure and functions” is also gratefully acknowledged.

T.O.C.

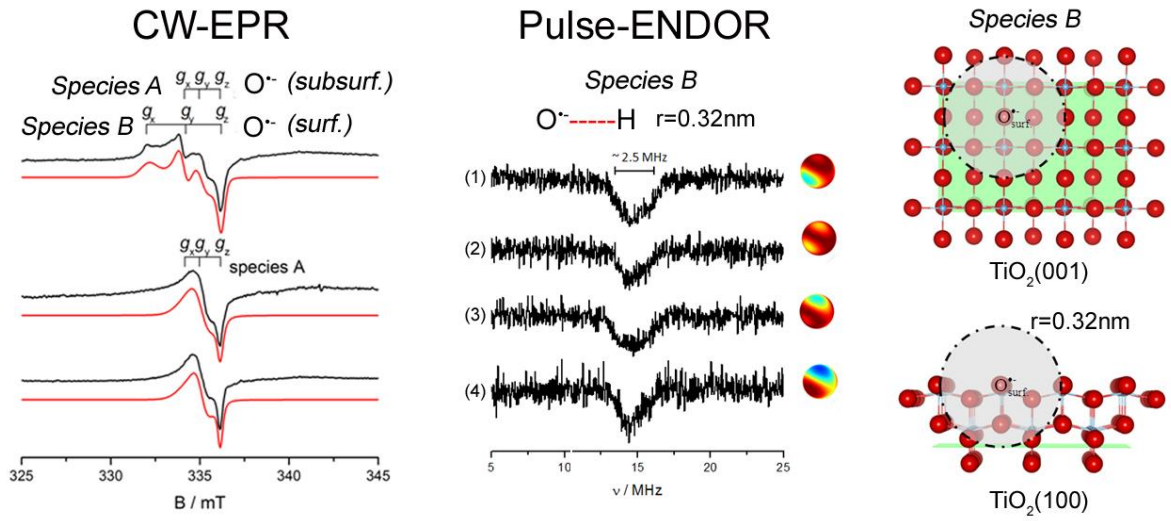

References.

[1] X. Chen, S.S. Mao, Titanium Dioxide Nanomaterials: Synthesis, Properties, Modifications, and Applications.Chem. Rev. 107 (2007) 2891-2959.

[2] J. Schneider, M. Matsuoka, M. Takeuchi, J. Zhang, Y. Horiuchi, M. Anpo, D. W. Bahnemann, Understanding TiO_2 Photocatalysis: Mechanisms and Materials. Chem. Rev. 114 (2014) 9919−9986.

[3] T.L. Thompson, J.T. Yates Jr., Surface Science Studies of the Photoactivation of TiO_2 New Photochemical Processes. Chem. Rev. 106 (2006) 4428−4453.

[4] A.Y. Nosaka, T. Fujiwara, H. Yagi, H. Akutsu, Y. Nosaka, Photocatalytic Reaction Sites at the TiO_2 Surface as Studied by Solid-State 1H NMR Spectroscopy. Langmuir 19 (2003) 1935-1937.

[5] M. A. Henderson, Effect of coadsorbed water on the photodecomposition of acetone on TiO2(110). J. Catal. 256 (2008) 287–292.

[6] K.L. Miller, C.W. Lee, J.L. Falconer, J.W. Medlin, Effect of water on formic acid photocatalytic decomposition on TiO_2 and Pt/TiO_2. J. Catal. 275 (2010) 294–299.

[7] M.A. Henderson, A Surface Science Perspective on TiO_2 Photocatalysis. Surf. Sci. Rep. 66 (2011) 185–297.

[8] S. Livraghi, I. Corazzari, M. C. Paganini, G. Ceccone, E. Giamello, B. Fubinia , I. Fenoglio, Decreasing the oxidative potential of TiO_2 nanoparticles through modification of the surface with carbon: a new strategy for the production of safe UV filters. Chem. Commun. 46 (2010) 8478–8480.

[9] P. Salvador, On the Nature of Photogenerated Radical Species Active in the Oxidative Degradation of Dissolved Pollutants with TiO_2 Aqueous Suspensions: A Revision in the Light of the Electronic Structure of Adsorbed Water. J. Phys. Chem. C 111 (2007) 17038-17043.

[10] A. Migani, D. J. Mowbray, J. Zhao, H. Petek, Quasiparticle Interfacial Level Alignment of Highly Hybridized Frontier Levels: H_2O on TiO_2(110). J. Chem. Theory Comput. 11 (2015) 239−251.

[11] E. Bae, N. Murakami, T. Ohno, Exposed Crystal Surface-controlled TiO_2 Nanorods Having Rutile Phase From $TiCl_3$ Under Hydrothermal Conditions. J. Mol. Catal. A: Chem. 300 (2009) 72–79.

[12] N. Murakami, Y. Kurihara, T. Tsubota, T. Ohno, Shape-Controlled Anatase Titanium(IV) Oxide Particles Prepared by Hydrothermal Treatment of Peroxo Titanic Acid in the Presence of Polyvinyl Alcohol. J. Phys. Chem. C 113 (2009) 3062–3069.

[13] T. Tachikawa, S. Yamashita, T. Majima, Evidence for Crystal-Face-Dependent TiO_2 Photocatalysis from Single-Molecule Imaging and Kinetic Analysis. J. Am. Chem. Soc. 133 (2011) 7197–7204.

[14] D.W. Bahnemann, M. Hilgendorff, R. Memming, Charge Carrier Dynamics at TiO_2 Particles: Reactivity of Free and Trapped Holes. J. Phys. Chem. B 101 (1997) 4265-4275.

[15] S. Kerisit, N.A. Deskins, K.M. Rosso, M. Dupuis, A Shell Model for Atomistic Simulation of Charge Transfer in Titania. J. Phys. Chem. C 112 (2008) 7678-7688.

[16] P. Zawadzki, Absorption Spectra of Trapped Holes in Anatase TiO_2. J. Phys. Chem. C 117 (2013) 8647−8651.

[17] R.F. Howe, M. Grätzel, EPR Study of Hydrated Anatase under UV Irradiation. J. Phys. Chem. 91 (1987) 3906-3909.

[18] O.I. Micic, Y. Zhang, K.R. Cromack, A.D. Trifunac, M.C. Thurnauer, Trapped Holes on $Ti0_2$ Colloids Studied by Electron Paramagnetic Resonance. J. Phys. Chem. 97 (1993) 1211-1283.

[19] Y. Nakaoka, Y. Nosaka, ESR Investigation into the Effects of Heat Treatment and Crystal Structure on Radicals Produced over Irradiated $Ti0_2$ Powder. J. Photochem. Photobiol. A 110 (1997) 299-305.

[20] H-H. Lo, N.O. Gopal, S-C. Sheu, S-C. Ke, Electron Paramagnetic Resonance Investigation of Charge Transfer in TiO_2(B)/Anatase and N−TiO_2(B)/Anatase Mixed-Phase Nanowires: The Relative Valence and Conduction Band Edges in the Two Phases. J. Phys. Chem. C 118 (2014) 2877−2884.

[21] N.M. Dimitrijevic, Z.V. Saponjic, B.M. Rabatic, O.G. Poluektov, T. Rajh, Effect of Size and Shape of Nanocrystalline TiO_2 on Photogenerated Charges. An EPR Study. J. Phys. Chem. C 111 (2007) 14597-14601.

[22] J.M. Coronado, A.J. Maira, J.C. Conesa, K.L. Yeung, V. Augugliaro, J. Soria, EPR Study of the Surface Characteristics ofNanostructured TiO_2 under UV Irradiation. Langmuir 17 (2001) 5368-5374.

[23] S-C. Ke, T-C. Wang, M-S. Wong, N.O. Gopal, Low Temperature Kinetics and Energetics of the Electron and Hole Traps in Irradiated TiO_2 Nanoparticles as Revealed by EPR Spectroscopy. J. Phys. Chem. B 110 (2006) 11628-11634.

[24] R. Scotti, M. D'Arienzo, A. Testino, F. Morazzoni, Photocatalytic Mineralization of Phenol catalyzed by Pure and Mixed Phase Hydrothermal Titanium Dioxide. Appl. Catal. B 88 (2009) 497–504.

[25] N.O. Gopal,; H-H. Lo, S-C. Sheu, S-C. Ke, A Potential Site for Trapping Photogenerated Holes on Rutile TiO_2 Surface as Revealed by EPR Spectroscopy: An Avenue for Enhancing Photocatalytic Activity. J. Am. Chem. Soc. 132 (2010) 10982–10983.

[26] S. Yang, A.T. Brant, L.E. Halliburton, Photoinduced self-trapped hole center in TiO_2 crystals. Phys. Rrv. B 82 (2010) 035209.

[27] V. Brezová, Z. Barbieriková, M. Zukalová, D. Dvoranová, L. Kavan, EPR study of17O-enriched titania nanopowders under UV irradiation. Catal. Today 230 (**2014)** 112–118.

[28] S. Livraghi, M. Chiesa, M.C. Paganini, E. Giamello, On the Nature of Reduced States in Titanium Dioxide as Monitored by Electron Paramagnetic Resonance. I: The Anatase Case. J. Phys. Chem. C 115 (2011**)** 25413−25421.

[29] S. Livraghi, S. Maurelli, M.C. Paganini, M. Chiesa, E. Giamello, Probing the Local Environment of Ti^{3+} Ions in TiO_2 (Rutile) by 17O HYSCORE. Angew. Chem., Int. Ed. 50 (2011) 8038−8040.

[30] 30 M. Chiesa, M.C. Paganini, S. Livraghi, E. Giamello, Charge Trapping in TiO_2 Polymorphs as Seen by Electron Paramagnetic Resonance Spectroscopy. Phys. Chem. Chem. Phys. 15 (2013**)** 9435− 9447.

[31] S. Livraghi, M. Rolando, S. Maurelli,; M. Chiesa, M.C. Paganini, E. Giamello, Nature of Reduced States in Titanium Dioxide as Monitored by Electron Paramagnetic Resonance. II: Rutile and Brookite Cases. J. Phys. Chem. C 118 (2014) 22141−22148.

[32] V. Bolis, C. Busco, M. Ciarletta, C. Distasi, J. Erriquez, I. Fenoglio, S. Livraghi, S. Morel, Hydrophilic/hydrophobic features of TiO_2 nanoparticles as a function of crystal phase, surface area and coating, in relation to their potential toxicity in peripheral nervous system. J. Colloid Interface Sci. 369 (2012) 28–39.

[33] C. Morterra, An infrared spectroscopic study of anatase properties. Part 6. Surface hydration and strong Lewis acidity of pure and sulphate-doped preparations. J. Chem. Soc., Farad Trans. I 84 (1988) 1617-1637.

[34] S. Stoll, A. Schweiger, EasySpin, a Comprehensive Software Package for Spectral Simulation and Analysis in EPR. J. Magn. Reson. 178 (2006) 42−55.

[35] T. Berger, O. Diwald, E. Knoezinger, F. Napoli, M. Chiesa, E. Giamello, Hydrogen activation at TiO_2 anatase nanocrystals. Chem. Phys. 339 (2007) 138−145.

[36] S. Maurelli, M. Vishnuvarthan, G. Berlier, M. Chiesa, NH_3 and O_2 Interaction with Tetrahedral Ti^{3+} Ions Isomorphously Substituted in the Framework of TiAlPO-5. A Combined Pulse EPR, Pulse ENDOR, UV-Vis and FT-IR Study. Phys. Chem. Chem. Phys. 14 (2012) 987-995.

[37] J. R. Brailsford, J. R. Morton, Paramagnetic Resonance Spectrum of O^- Trapped in KCl, RbCl, and KBr. J. Chem. Phys. 51 (1969) 4794-4798.

[38] U. Diebold , The surface science of titanium dioxide. Surf. Sci. Rep. 48 (2003) 53-229.

[39] A. Selloni, Crystal growth: Anatase shows its reactive side. Nat. Mate. 7 (2008) 613-615.

[40] J. Blomquist, L.E. Walle, P. Uvdal,; A. Borg, A. Sandell, Water Dissociation on Single Crystalline Anatase TiO_2(001) Studied by Photoelectron Spectroscopy. J. Phys. Chem. C 112 (2008) 16616–16621.

[41] M. Horn, C.F. Schwerdtfeger, E. P. Meagher, Refinement of the structure of anatase at several temperatures Zeitschrift fur Kristallographie 136 (1972) 273-281.

[42] J. Lee, D.C. Sorescu, X. Deng, K.D. Jordan, Water Chain Formation on TiO_2(110). J. Phys. Chem. Lett. 4 (2013) 53–57.

[43] U. J. Aschauer, A. Tilocca, A. Selloni, Ab Initio Simulations of the Structure of Thin Water Layers on Defective Anatase TiO_2(101) Surfaces. Int. J. Quantum Chem. 115 (2015) 1250-1257.